THE JOURNAL OF BIOLOGICAL CHEMISTRY
Vol. 278, No. 18, Issue of May 2, pp. 16222–16229, 2003
Printed in U.S.A.

A Novel TRPM2 Isoform Inhibits Calcium Influx and Susceptibility to Cell Death*

Received for publication, January 19, 2003, and in revised form, February 18, 2003
Published, JBC Papers in Press, February 19, 2003, DOI 10.1074/jbc.M300298200

Wenyi Zhang‡, Xin Chu‡, Qin Tong‡, Joseph Y. Cheung‡§, Kathleen Conrad‡, Kathryn Masker‡, and Barbara A. Miller‡¶‖

From the ‡Henry Hood Research Program, The Sigfried and Janet Weis Center for Research and the Departments of §Medicine and ¶Pediatrics, The Geisinger Clinic, Danville, Pennsylvania 17822

TRPM2 is a Ca^{2+}-permeable channel that is activated by oxidative stress and confers susceptibility to cell death. Here, an isoform of TRPM2 was identified in normal human bone marrow that consists of the TRPM2 N terminus and the first two predicted transmembrane domains. Because of alternative splicing, a stop codon (TAG) is located at the splice junction between exons 16 and 17, resulting in deletion of the four C-terminal transmembrane domains, the putative calcium-permeable pore region, and the entire C terminus. This splice variant was found in other hematopoietic cells including human burst forming unit-erythroid-derived erythroblasts and TF-1 erythroleukemia cells. Endogenous expression of both the short form of TRPM2 (TRPM2-S) and the full length (TRPM2-L) was determined by reverse transcriptase-PCR, and localization of endogenous TRPM2 to the plasma membrane was demonstrated by confocal microscopy. Heterologous expression of TRPM2-S in HEK 293T cells demonstrated similar membrane localization as TRPM2-L, and coexpression of TRPM2-S did not alter the subcellular localization of TRPM2-L. The direct interaction of TRPM2-S with TRPM2-L was demonstrated with immunoprecipitation. H_2O_2 induced calcium influx through TRPM2-L expressed in 293T cells. Coexpression of TRPM2-S suppressed H_2O_2-induced calcium influx through TRPM2-L. Furthermore, expression of TRPM2-S inhibited susceptibility to cell death and onset of apoptosis induced by H_2O_2 in cells expressing TRPM2-L. These data demonstrate that TRPM2-S is an important physiologic isoform of TRPM2 and modulates channel activity and induction of cell death by oxidative stress through TRPM2-L.

Regulation of the intracellular calcium concentration $[Ca^{2+}]_i$ is of critical importance in determination of cell fate. In many cell types, oxidative stress, through the production of oxygen metabolites including H_2O_2, causes an increase in $[Ca^{2+}]_i$, which results in cell injury, apoptosis, or necrosis (1, 2). One mechanism through which H_2O_2 may disrupt calcium homeostasis has recently been identified. A widely expressed Ca^{2+}-permeable cation channel, TRPM2, can be activated by micromolar levels of H_2O_2 and other agents that produce reactive oxygen species (3, 4). This channel is part of a physiological pathway through which H_2O_2 and tumor necrosis factor α may induce cell death (3).

TRPM2, also called LTRPC-2 or TRPC7, is a member of the transient receptor potential (TRP)[1] protein superfamily. This is a diverse group of calcium-permeable cation channels expressed on nonexcitable cells, related to the archetypal TRP, *Drosophila* Trp (5–7). The TRP superfamily, conserved from *Caenorhabditis elegans* to humans, has been divided into six subfamilies. Mammalian isoforms share six putative transmembrane domains similar to the core structure of many pore-forming subunits of voltage-gated channels except that they lack positively charged residues necessary for the voltage sensor. One subfamily of TRP channels are referred to as TRPMs (3, 4, 8–14), because the first described member was melastatin (MLSN), a putative tumor suppressor protein (6, 7). Prior to implementation of a unified nomenclature for the TRP superfamily, this subfamily was also known as LTRPC, named because of longer open reading frames of ~1600 amino acids (5). Although the mechanisms of activation of specific TRPM are not known, some TRPM appear to have important roles in cell proliferation. For example, TRPM1 (MLSN) is expressed in melanocytes, and its level of expression correlates inversely with melanoma aggressiveness and the potential for melanoma metastasis (8, 9). TRPM5 (MTR1 and LTRPC5) is located in the Beckwith-Wiedemann syndrome critical region of human chromosome 11, although its function in cell growth is not known (12, 15). TRPM8 (Trp-p8) has significant homology to human melastatin, but it is up-regulated in prostate cancer and a number of nonprostatic neoplastic tumors (13).

TRPM2 has been cloned from human brain, lymphocytes, and monocytes (11, 16, 17). TRPM2 is activated by H_2O_2 and other agents that produce reactive oxygen species, resulting in an increase in the intracellular free calcium concentration ($[Ca^{2+}]_i$) (3, 4). Heterologous expression of TRPM2 in 293 cells conferred susceptibility to H_2O_2-induced cell death, which correlated with the elevation in $[Ca^{2+}]_i$. Furthermore, suppression of endogenous TRPM2 expression in rat insulinoma RIN-5F or monocyte U937 cells resulted in significantly diminished Ca^{2+} influx and cell death induced by H_2O_2 or tumor necrosis factor α (3). These data strongly support the physiologic role of TRPM2 as an endogenous H_2O_2-activated calcium-permeable channel that mediates cell death following oxidative stress.

In this report, a truncated isoform of TRPM2 was identified

* This work was supported by National Institutes of Health Grants DK 46778 (to B. A. M.) and HL 58672 (to J. Y. C.) and grants from the Geisinger Foundation. The costs of publication of this article were defrayed in part by the payment of page charges. This article must therefore be hereby marked "*advertisement*" in accordance with 18 U.S.C. Section 1734 solely to indicate this fact.

‖ To whom correspondence should be addressed: The Henry Hood Research Program, The Sigfried and Janet Weis Center for Research, Geisinger Clinic, 100 North Academy Ave., Danville, PA 17822-2616. Tel.: 570-271-6675; Fax: 570-271-6701; E-mail: bamiller1@geisinger.edu.

[1] The abbreviations used are: TRP, transient receptor potential; BFU-E, burst forming unit-erythroid; GFP, green fluorescent protein; BFP, blue fluorescent protein; FBS, fetal bovine serum; PI, propidium iodide; CMV, cytomegalovirus; RT, reverse transcriptase; MLSN, melastatin.

in human hematopoietic cells that lacks four of the six predicted C-terminal transmembrane domains and the putative pore region permeable to calcium. The short form of TRPM2 (TRPM2-S) was determined to interact directly with full-length (TRPM2-L). Using a digital video imaging system in which single 293T cells that express transfected TRPM2-S were identified by detection of green fluorescent protein (GFP), cells that express transfected TRPM2-L were identified by detection of blue fluorescent protein (BFP), and $[Ca^{2+}]_i$ was simultaneously measured by Fura Red fluorescence, the ability of TRPM2-S to suppress H_2O_2-induced calcium influx through TRPM2-L was demonstrated. In addition, the short form of TRPM2 inhibited susceptibility to cell death induced by H_2O_2 through full-length TRPM2. These data suggest that the interaction between TRPM2-S and TRPM2-L is an important mechanism for regulating channel activity as well as the cellular response to oxidative stress.

EXPERIMENTAL PROCEDURES

Culture of Cell Lines and Human BFU-E-derived Cells—Jurkat cells, K562, AML-193, and TF-1 cells were obtained from the American Type Culture Collection (Manassas, VA). Jurkat cells were cultured in RPMI 1640 medium with 10% fetal bovine serum (FBS). K562 cells were cultured in Iscove's modified Dulbecco's medium with 10% FBS. AML-193 cells were cultured in Iscove's modified Dulbecco's medium with 0.005 mg/ml insulin, 0.005 mg/ml transferrin, 5 ng/ml granulocyte-macrophage colony-stimulating factor, and 5% FBS. TF-1 cells were cultured in RMPI 1640 medium with 1 ng/ml granulocyte-macrophage colony-stimulating factor. HEK 293 cells were obtained from the American Type Culture Collection, and 293T cells were obtained from Dr. Dwayne Barber (Ontario Cancer Institute, Toronto, Canada). Both were cultured in Dulbecco's modified Eagle's medium with 10% FBS. Peripheral blood from volunteer donors was obtained under protocols approved by the Geisinger Institutional Review Board. Human BFU-E were cultured in methyl cellulose medium, and BFU-E-derived cells were harvested at day 10 as described previously (18).

RT-PCR of TRPM2 in Human Primary Cells and Cell Lines—RNA was prepared from human 293T, Jurkat, K562, AML-193, TF-1 cells, and BFU-E-derived cells. cDNA was prepared from RNA using the Superscript First Strand Synthesis System (Invitrogen) for RT-PCR. RT-PCR was performed for 35 cycles (denaturation at 94 °C for 30 s, annealing at 57 °C for 30 s, and extension at 72 °C for 30 s). Primers for TRPM2 were 5′ primer (5′-TCGGACCCAACCACACGCTGTA-3′) and 3′ primer (5′-CGTCATTCTGGTCCTGGAAGTG-3′). Control 18 S rRNA primers used in RT-PCR were 5′ primer (5′-GAAAGT CGGAGGTTCG-AAGA-3′) and 3′ primer (5′-ACCAACTAAGAACGGCCTG-3′).

Cloning of TRPM2-L and TRPM2-S—TRPM2 was cloned from human bone marrow Marathon-Ready cDNA (Clontech, Palo Alto, CA) by amplifying five adjacent cDNA fragments encoding the complete open reading frame of TRPM2 with five PCR reactions. The primers were chosen based on the published cDNA sequence of TRPM2 (GenBank™ accession number AB001535). For the first fragment, the primers were chosen to amplify the region between nucleotides 361 and 1572 (1447-nucleotide *Sma*I site); the second fragment was amplified with primers to the region between nucleotides 1350 and 2442 (1447-nucleotide *Sma*I and 2299-nucleotide *Nco*I sites); the third fragment was amplified with primers to the region between nucleotides 2261 and 3376 (2299-nucleotide *Nco*I and 3358-nucleotide *Acc*I sites); the fourth fragment was amplified with primers to the region between nucleotides 3351 and 4351 (3358-nucleotide *Acc*I and 4294-nucleotide *Not*I sites); and the fifth fragment was amplified with primers to the region between nucleotides 4243 and 5138 (4294-nucleotide *Not*I site and 4955-nucleotide stop codon). Each of these five fragments was sequenced following T/A cloning.

Fragments 1–5 representing the published sequence of TRPM2 were cloned into pUC18 following appropriate restriction enzyme digestion to yield TRPM2-L (4.8 kb). The first segment was subcloned into pUC18 following restriction digestion with *Hin*dIII and *Sma*I. The second segment was ligated into pUC18 containing the first segment using the *Sma*I and *Eco*RI sites. The third segment was subcloned into pUC18 containing the first and second segments at the *Nco*I and *Eco*RI sites. The fourth segment was separately subcloned into pUC18 using the *Acc*I and *Eco*RI restriction digestion sites, and the fifth segment was ligated into pUC18 containing the fourth segment at the *Not*I site. Subsequently, the fourth and fifth segments were subcloned into pUC18 containing the first, second, and third segments at *Acc*I and *Eco*RI. For the short version TRPM2-S (3.0 kb), fragments 1–3 representing the isoform with the stop codon in the third fragment were cloned into pUC18 using the same restriction enzyme strategy described for TRPM2-L.

Expression of TRPM2-L and TRPM2-S—For expression studies, TRPM2-L and TRPM2-S were subcloned from pUC18 into pcDNA3.1 (Invitrogen) and into pET-42b (Novagen, Madison, WI). TRPM2-L and TRPM2-S were also subcloned into pcDNA3.1/V5-His TOPO (Invitrogen) following amplification by PCR. For digital video imaging studies, TRPM2-L was subcloned into pQBI50 (QbioGene, Carlsbad, CA) and TRPM2-S into pTracer-CMV (Invitrogen).

To demonstrate the presence of TRPM2-S in TF-1 cells and BFU-E derived cells, RNA was prepared from these cells, and cDNA was synthesized as described above for RT-PCR. PCR was used to amplify the third fragment between nucleotides 2261 and 3376 using the 5′ primer (5′-TCCCTCTACAAGCGTTCCTCAG-3′) and the 3′ primer (5′-GGTGAGGTAGGAGTGGTAGACG-3′). The PCR products were subcloned into the T/A vector, and the insert was sequenced to confirm the presence or absence of the TAG stop codon.

Generation of Antibodies Specific to TRPM2—Two rabbit polyclonal antibodies were generated to TRPM2 and affinity-purified by Bethyl Laboratories (Montgomery, TX). One of these antibodies (anti-TRPM2-N) was generated to an epitope in the N terminus of TRPM2 (ILKELSKEEEDTDSSEEMLA, amino acids 658–677) and recognized both TRPM2-L and TRPM2-S. A second antibody (anti-TRPM2-C) was generated to an epitope in the C terminus of TRPM2 (KAAEEPDAEPG-GRKKTEEPGDS, amino acids 1216–1237) and was specific for TRPM2-L. Specificity of the antibodies was confirmed using *in vitro* translation products prepared with cDNAs for mTRPC2 clone 14 (19), hTRPC6 (20), TRPM2-S, and TRPM2-L, cloned into pcDNA3 or pcDNA3.1/V5-His TOPO vector as described previously (21). The *in vitro* translation products were prepared with the TNT quick coupled transcription/translation system (Promega, Madison, WI).

Immunoblotting of Whole Cell Lysates and Crude Membrane Preparations—Human 293T cells were transiently transfected using LipofectAMINE PLUS Reagent with vector alone, TRPM2-S, TRPM2-L, or both, in pcDNA3.1 or pcDNA3.1/V5-His TOPO. The cells were routinely studied 48 h after transfection. For Western blotting of whole cell lysates, the lysates were separated on 8% polyacrylamide gels, followed by transfer to polyvinylidene difluoride membranes. Following blocking, the blots were incubated with primary antibody (anti-TRPM2-N, 1:300; anti-TRPM2-C, 1:500; anti-V5, 1:2000 (Invitrogen); anti-TRPC6, 1:200 (Alomone Laboratories, Jerusalem, Israel)), washed, and then incubated with horseradish peroxidase-conjugated anti-rabbit or anti-mouse antibody (1:2000). ECL was used for detection of signal. The crude membranes were also prepared from 293T cell pellets transfected with vector alone (pcDNA3.1), TRPM2-S, and/or TRPM2-L as described previously (21), and Western blotting was performed as described above.

Immunoprecipitation—To determine whether anti-TRPM2-N and anti-TRPM2-C antibodies are able to immunoprecipitate their targets, TRPM2-S and TRPM2-L proteins were prepared from TRPM2-S and TRPM2-L cDNAs subcloned into pET-42b and expressed with the TNT quick coupled transcription/translation system. *In vitro* translation was performed with labeling using Transcend™ Biotin-Lysyl-tRNA. TRPM2-S and TRPM2-L *in vitro* translated proteins were incubated with anti-TRPM2-N or anti-TRPM2-C antibodies overnight at 4 °C. Protein A-Sepharose 4 Fast Flow (Amersham Biosciences) was then added for 30 min, followed by washing and then boiling of beads to remove precipitated protein. Western blotting was performed with the supernatant and with pelleted proteins as described above, except that horseradish peroxidase-streptavidin was used for the detection of positive signals.

To determine whether TRPM2-L interacts directly with TRPM2-S, 293T cells were transfected with empty vector (pcDNA3.1), TRPM2-S in pcDNA3.1/V5-His TOPO, TRPM2-L in pcDNA3.1, or both. The lysates were prepared from cell pellets and preabsorbed with protein A/G-agarose. 500 μg of each supernatant was incubated with anti-TRPM2-C (20 μg) or anti-V5 (5 μg) antibodies at 4 °C overnight. Protein A/G-agarose was then added, the immunoprecipitates were washed, and Western blotting was performed as described above.

Immunolocalization of TRPM2 in TF-1 Erythroleukemia Cells and in Transfected 293T Cells—TF-1 cells were placed in each well of Lab-Tek Permanox Chamber Slides precoated with fibronectin. After 30 min, the cells were washed three times with phosphate-buffered saline, fixed with methanol at −20 °C for 10 min, and permeabilized in 0.5% Triton X-100 in phosphate-buffered saline for 5 min. Incubation for 10 min in

20% goat serum preceded staining with primary antibody (anti-TRPM2-N or anti-TRPM2-C, 1:50) for 20 min at room temperature, followed by secondary antibody (goat anti-rabbit Alexa 488; Molecular Probes, Eugene, OR) for 20 min in the dark. The slides were stained with propidium iodide (PI) in Vectashield mounting medium (Vector Laboratories, Burlingame, CA). The images were acquired with a Leica TCS SP2 Confocal Microscope.

293T cells transfected with TRPM2-L in pcDNA3.1, TRPM2-S in pcDNA3.1/V5-His TOPO, or both were plated on polylysine-coated chamber slides 24 h after transfection and incubated for 24 h more at 37 °C. The cells were fixed, permeabilized, and incubated with primary (rabbit anti-TRPM2-C or mouse anti-V5) or secondary antibodies (fluorescein isothiocyanate donkey anti-rabbit IgG; Jackson Laboratories, West Grove, PA; Texas Red goat anti-mouse) as described above. The slides were stained with DAPI in Vectashield mounting medium to visualize DNA instead of PI, which could not be distinguished from Texas Red fluorescence. To visualize DAPI, the cells were viewed using a Nikon Opiphot-2 microscope equipped for epifluorescence. The images were acquired with an air-cooled CCD SenSys digital camera from Photometrics (Tuscon, AZ) and processed using IPLab and Enhanced Photon Reassignment software programs obtained from Scanalytics (Fairfax, VA).

Measurement of $[Ca^{2+}]_i$ with Digital Video Imaging—293T cells were transfected with TRPM2-S subcloned into pTracer-CMV, TRPM2-L subcloned into pQBI50, or both as described above. The pTracer-CMV vector contains an SV40 promoter driving expression of a GFP gene and a CMV promoter driving expression of TRPM2-S. The pQBI50 vector contains a CMV promoter that drives expression of SuperGlo BFP fused through a flexible linker to TRPM2-L. Successful transfection of 293T cells with TRPM2-S and TRPM2-L was verified by detection of GFP (excitation, 478 nm; emission, 535 nm) and BFP (excitation, 380 nm; emission 435 nm), respectively, in cells with our digital video imaging system (21, 22). The fluorescence microscopy-coupled digital video imaging used to measure changes in $[Ca^{2+}]_i$ has been described previously (22–25). To study changes in $[Ca^{2+}]_i$ in transfected cells, we were not able to use Fura-2 as the detection fluorophore because its excitation and emission wavelengths overlap with those of GFP. Instead, we used the fluorescent indicator Fura Red (excitation, 460 and 490 nm; emission, 600-nm-long pass), a dual wavelength excitation probe. We determined R_{min} (minimum fluorescence intensity ratio (r) of the emission following excitation at 460 nm divided by the emission following excitation at 490 nm), R_{max} (maximum r), and the constants S_{f2}/S_{b2} with Fura Red so that $[Ca^{2+}]_i$ could be calculated using the formula $[Ca^{2+}]_i = K'_D[(R - R_{min})/(R_{max} - R)]\ (S_{f2}/S_{b2})$.

Transfected 293T cells grown on glass coverslips were loaded at 48 h with 5 μM Fura Red-AM for 30 min at 37 °C in the presence of Pluronic F-127 to enhance loading. Transfected 293T cells were treated with 0–10 mM H_2O_2 and $[Ca^{2+}]_i$ measured at base line and over a 20-min interval. Statistical significance of results was analyzed with one-way analysis of variance.

Assays of Cell Viability—293T cells transfected for 48 h with vector, TRPM2-S, TRPM2-L, or both in pQBI50 were treated with 0–10 mM H_2O_2 for 40 min. Cell viability was assessed by trypan blue exclusion. Induction of apoptosis or necrosis was also assessed in these cells following treatment with H_2O_2 with the Vibrant apoptosis assay kit 2 (Molecular Probes), in which apoptotic cells are labeled with annexin V conjugated to Alexa Fluor 488 and necrotic cells are labeled with propidium iodide.

RESULTS

Cloning of TRPM2-S—TRPM2 has been reported to be highly expressed in lymphocytes as well as in granulocytes and other hematopoietic cell lines (4, 17). To study TRPM2 in human hematopoietic cells, the expression of TRPM2 in different hematopoietic lineages was first examined. RT-PCR was performed on RNA isolated from Jurkat (T cell lymphoblast cell line), K562 (chronic myelogenous leukemia cell line), AML-193 (acute monocytic leukemia cell line), and TF-1 (erythroleukemia cell line) cells and from BFU-E-derived primary erythroid cells (18). The results are shown in Fig. 1. TRPM2 mRNA was highly expressed in Jurkat, K562, AML-193, and TF-1 cells. TRPM2 was also expressed, although at lower levels, in primary human erythroblasts at day 10 of culture, which are largely proerythroblasts (18). TRPM2 mRNA was detectable at low levels in 293 cells; these results differ from a previous report in which TRPM2 mRNA was undetectable in 293 cells (17), possibly because of differences in the RT-PCR conditions or in the 293 cells studied. No TRPM2 bands were observed when PCR was performed without the reverse transcriptase step, demonstrating that these products did not result from contaminating DNA. The identity of PCR bands was confirmed by sequencing.

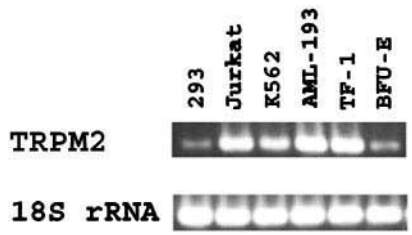

FIG. 1. **RT-PCR of TRPM2 in human hematopoietic cells.** RT-PCR was performed on RNA isolated from 293, Jurkat, K562, AML-193, and TF-1 cell lines and from BFU-E-derived erythroblasts at day 10 of culture. 18 S rRNA primers were used as a control.

To clone TRPM2 for further study, a strategy was designed based on the published cDNA sequence (see "Experimental Procedures"). Using Marathon-Ready cDNA from human bone marrow as the template, five adjacent cDNA fragments encoding the complete open reading frame of TRPM2 were amplified by PCR. Following sequencing, the fragments were ligated together to produce full-length TRPM2 (TRPM2-L). Sequencing of the third fragment resulted in two alternative sequences; one was identical to the published sequence, and the other included a TAG stop codon at nucleotides 2984–2986. This sequence is a result of alternative splicing of the 3′ end of the intron between exons 16 and 17. As shown on Fig. 2, this isoform, TRPM2-S, results in the deletion of the entire C terminus of full-length TRPM2, including the four C-terminal transmembrane domains and the putative pore region permeable to calcium. Because the TAG stop codon immediately follows the CAG encoding glutamine (Fig. 2), no unique amino acids are introduced in the TRPM2-S protein.

The PCR products following amplification of bone marrow cDNA with primers for the third fragment of TRPM2 were subcloned into the T/A vector, and 13 clones were sequenced. The sequences of seven different clones were identical to TRPM2-S, and six were identical to TRPM2-L. To determine whether TRPM2-S is expressed in other hematopoietic cells, cDNA was also prepared with RNA from normal human BFU-E-derived cells and from TF-1 cells. As described above, PCR products amplified with primers for the third fragment were subcloned into the T/A vector, and the clones were sequenced. Four of eight clones from normal human BFU-E derived cells, and two of three clones from TF-1 cells were identical to TRPM2-S; the rest were identical to TRPM2-L. These data demonstrate the presence of TRPM2-S in three different hematopoietic cell types.

Generation of Antibodies Specific to TRPM2—To study the interaction and function of TRPM2 isoforms, an affinity-purified antibody was generated to the N terminus of TRPM2 (anti-TRPM2-N), which recognizes both TRPM2-S and TRPM2-L. A second antibody was generated to the C terminus of TRPM2 (anti-TRPM2-C), which recognizes only TRPM2-L. To characterize antibody specificity, *in vitro* translation was performed using cDNAs for TRPM2-S and TRPM2-L in pcDNA3.1/V5-His TOPO and mTRPC2 clone 14 and hTRPC6 in pcDNA3 as controls. Western blotting was performed with each of these *in vitro* translation products with anti-TRPM2-N, anti-TRPM2-C, anti-V5, or anti-TRPC6 antibodies. The results are shown in Fig. 3*A*. Anti-TRPM2-N recognized the *in vitro* translation products TRPM2-S (95

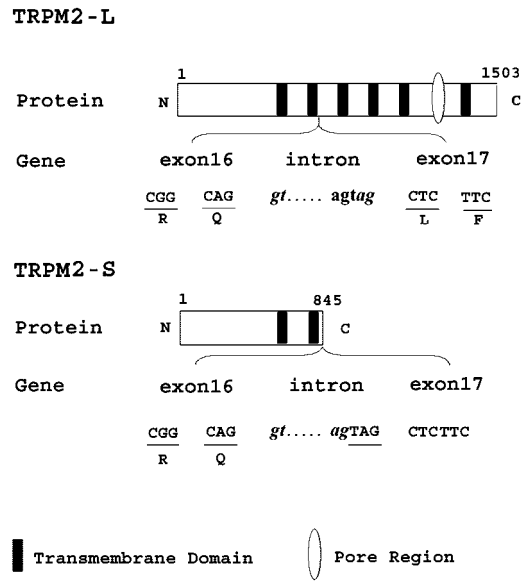

FIG. 2. **Schema of cDNA for the two splice variants TRPM2-L and TRPM2-S.** The protein structures of TRPM2-L and TRPM2-S are shown with the predicted transmembrane domains and the pore region indicated. Nucleotide and amino acid sequences surrounding the alternatively spliced stop codon between exons 16 and 17 are shown below the TRPM2 gene, demonstrating termination of TRPM2 after the second transmembrane domain in TRPM2-S.

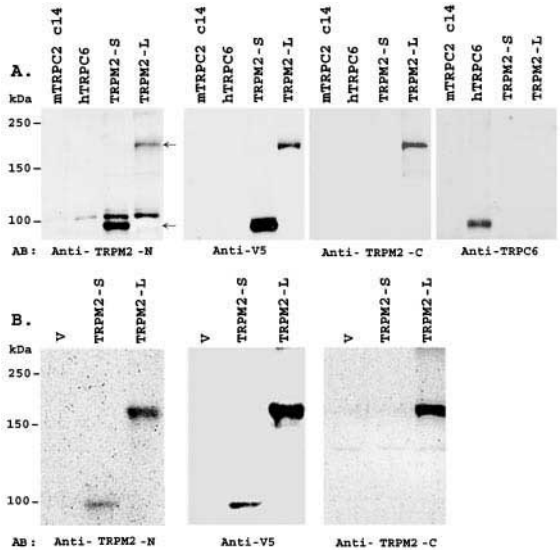

FIG. 3. *A*, specificity of TRPM2 antibodies. *In vitro* translation products were prepared using cDNAs of mTRPC2 clone 14 (pcDNA3), hTRPC6 (pcDNA3), and TRPM2-S and TRPM2-L in pcDNA3.1/V5-His TOPO. Equivalent amounts of each reaction were loaded in each lane, and Western blotting was performed. The blots were probed with anti-TRPM2-N, anti-V5, anti-TRPM2-C, and anti-TRPC6 antibodies (*AB*). *B*, Western blot of transfected 293T cells. The lysates were prepared from 293T cells transfected with empty vector, TRPM2-S, and TRPM2-L. Equivalent amounts of protein were loaded in each lane. The blots were probed with anti-TRPM2-N, anti-V5, and anti-TRPM2-C antibodies.

kDa) and TRPM2-L (171 kDa), both with tags that add ~6 kDa to the predicted molecular masses. A nonspecific cross-reacting band was observed at 105 kDa with anti-TRPM2-N antibody. Anti-V5 recognized the tagged *in vitro* translation products TRPM2-S and TRPM2-L. Anti-TRPM2-C recognized only TRPM2-L. Anti-TRPC6 was used as a control to demonstrate the presence of the *in vitro* translation product hTRPC6 (100 kDa) on the blots. The presence of TRPC2 clone 14 (132 kDa) was also confirmed as previously (Ref. 21 and results not shown). Neither anti-TRPM2-N or anti-TRPM2-C

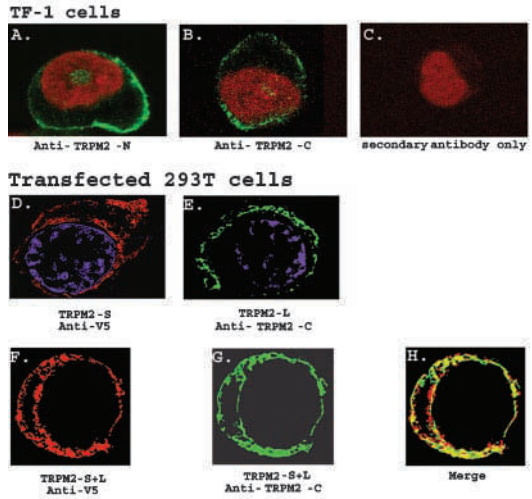

FIG. 4. **Immunofluorescence of TRPM2 in TF-1 and in transfected 293T cells.** TF-1 cells fixed to glass slides were stained with anti-TRPM2-N and secondary antibody (*A*), anti-TRPM2-C and secondary antibody (*B*), or secondary goat anti-rabbit Alexa 488 antibody alone (*C*). PI was used to stain DNA (*A–C*). *D*, 293T cells transfected with TRPM2-S were stained with anti-V5 as the primary antibody and Texas Red anti-mouse IgG as the secondary antibody. DAPI was used to stain DNA. *E*, 293T cells transfected with TRPM2-L were stained with anti-TRPM2-C and fluorescein isothiocyanate anti-rabbit secondary antibodies. 293T cells transfected with both TRPM2-S and TRPM2-L were stained with anti-V5 and goat anti-mouse secondary antibodies (*F*) and anti-TRPM2-C and donkey anti-rabbit secondary antibodies (*G*). The merged images of *F* and *G* are shown in *H* and demonstrate significant overlap.

antibodies recognized mTRPC2 or hTRPC6.

293T cells were then transfected with vector alone, TRPM2-S, or TRPM2-L in pcDNA3.1/V5-His TOPO. The cell lysates were prepared, and Western blotting was performed. Fig. 3*B* demonstrates the ability of anti-TRPM2-N to specifically recognize TRPM2-S and TRPM2-L and the ability of anti-TRPM2-C to recognize TRPM2-L in transfected cells. These observations were confirmed with antibody directed to the V5 tag. Fig. 3*B* also demonstrates the inability to detect endogenous TRPM2 protein expression in 293T cells under the identical conditions, suggesting that endogenous protein levels are low or absent.

Expression of Endogenous TRPM2—To confirm the expression and determine the subcellular localization of endogenous TRPM2, immunolocalization studies were performed with TF-1 cells using anti-TRPM2-N and anti-TRPM2-C antibodies and confocal microscopy. PI staining was used to localize DNA. Representative results shown here demonstrate that endogenous TRPM2 recognized by either anti-TRPM2-N (Fig. 4*A*) or anti-TRPM2-C (Fig. 4*B*) is localized on or near the plasma membrane. In Fig. 4*C*, no fluorescence was observed in control cells stained with secondary antibody alone. Unfortunately, anti-TRPM2-N antibodies cannot distinguish TRPM2-S from TRPM2-L; the amino acid sequence of TRPM2-S is identical to LTRCP2-L throughout the TRPM2-S sequence.

Subcellular Localization of TRPM2-S and TRPM2-L—To distinguish the subcellular localization of TRPM2-S or TRPM2-L isoforms and determine whether TRPM2-S alters the localization of TRPM2-L (10), 293T cells were transfected with TRPM2-S in pcDNA3.1/V5-His TOPO, TRPM2-L in pcDNA3.1, or both. TRPM2-S was detected with antibody to the V5 tag, and TRPM2-L was detected with antibody specific for the C terminus of TRPM2. Cell staining was visualized by fluorescence microscopy. The images at different planes through the cell were deconvolved (Scanalytics software) to remove out-of-focus contaminating light to generate high reso-

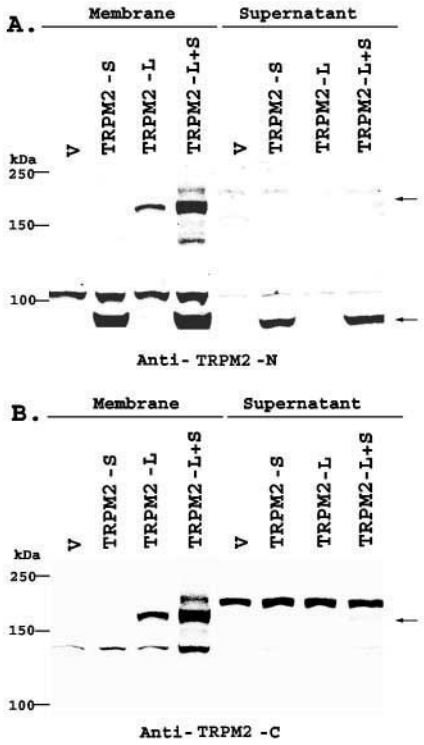

FIG. 5. **Membrane localization of TRPM2-S and TRPM2-L.** Western blots were performed on crude membrane pellets or the supernatants of 293T cells transfected with pcDNA3.1 vector alone (*V*), TRPM2-S, TRPM2-L, or both. The blots were probed with anti-TRPM2-N (*A*) or anti-TRPM2-C antibodies (*B*).

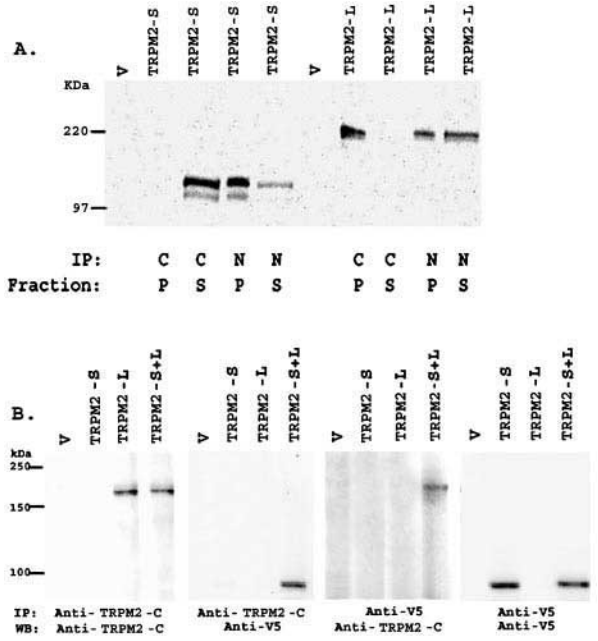

FIG. 6. **Interaction of TRPM2-S with TRPM2-L.** *A*, to demonstrate the ability of anti-TRPM antibodies to immunoprecipitate, *in vitro* translated proteins were prepared using empty vector or cDNAs of TRPM2-S or TRPM2-L in pET-42b and labeling with Transcend™ Biotin-Lysyl-tRNA. The proteins were immunoprecipitated with anti-TRPM2-C (*C*) or anti-TRPM2-N (*N*) antibodies, and Western blotting was performed with precipitated proteins (*P*) or supernatant before the first wash (*S*). The proteins were detected by horseradish peroxidase-streptavidin followed by ECL. *B*, 293T cells were transfected with vector alone (pcDNA3.1), TRPM2-S in pcDNA3.1/V5-His TOPO, TRPM2-L in pcDNA3.1, or both. The cell lysates were immunoprecipitated with anti-TRPM2-C or anti-V5 antibodies. Western blotting was performed with anti-TRPM2-C antibody, and the blots were then stripped and reprobed with anti-V5 antibody.

lution images. In 293T cells transfected with a single vector, TRPM2-S (Fig. 4*D*) or TRPM2-L (Fig. 4*E*) were expressed at or near the plasma membrane, as well as throughout the cytoplasm in a nonhomogeneous pattern. When TRPM2-S and TRPM2-L were coexpressed in the same 293T cells (Fig. 4, *F–H*), the expression pattern was not different from that observed when each was expressed alone, and the spatial distribution showed extensive overlap. The results were identical when a range of DNA concentrations was used to transfect 293T cells to reduce the level of expressed protein. The results were also similar when CHO, CHO-S, or COS-1 cells were transfected (not shown). When anti-V5, anti-TRPM2-N, or anti-TRPM2-C antibodies were used with the appropriate secondary antibody to stain 293T cells transfected with vector alone, no positive fluorescence was observed (not shown). These data show that transfected TRPM2-L and TRPM2-S are also expressed at or near the plasma membrane.

To confirm that TRPM2-S and TRPM2-L have a similar subcellular distribution and that TRPM2-S does not alter the subcellular localization of TRPM2-L, crude membrane fractions were prepared from 293T cells transfected with vector alone (pcDNA3.1), TRPM2-S, TRPM2-L, or both as described previously (21). Western blotting was performed with protein isolated in the crude membrane pellet or the supernatant, and the blots were probed with anti-TRPM2-N (Fig. 5*A*) or anti-TRPM2-C (Fig. 5*B*) antibodies. A protein band of ~171 kDa was observed in cells transfected with TRPM2-L, which localized to the membrane fraction. A protein band of ~95 kDa was observed in cells transfected with TRPM2-S, which also primarily localized to the membrane fraction. When coexpressed, both TRPM2-S and TRPM2-L continued to localize in the membrane fraction rather than in the supernatant. These data confirm that TRPM2-S does not alter the localization of TRPM2-L and that TRPM2-S and TRPM2-L have a similar subcellular localization. They also suggest that the nonhomogeneous cytoplasmic staining observed with immunofluorescent microscopy in 293T cells transfected with TRPM2-S or TRPM2-L (Fig. 4, *D–H*) represents intracellular membrane structures in which TRPM2 is produced or transported.

Direct Protein Interaction between TRPM2 Isoforms—To study the interaction of TRPM2 isoforms with each other, the ability of anti-TRPM2 antibodies to immunoprecipitate their targets was first examined. TRPM2-S and TRPM2-L cDNAs in pET-42b were expressed by *in vitro* translation and labeled using Biotin-Lysyl-tRNA. Each of these *in vitro* translation products was incubated with anti-TRPM2-C or anti-TRPM2-N antibodies and bound protein precipitated with protein A-Sepharose. Western blotting of pelleted fractions or the supernatants demonstrates that anti-TRPM2-C immunoprecipitates TRPM2-L but not TRPM2-S (Fig. 6*A*). The results also demonstrate that anti-TRPM2-N immunoprecipitates both TRPM2-S and TRPM2-L but that TRPM2-L is not immunoprecipitated as efficiently as TRPM2-S by this antibody. The higher molecular masses of proteins shown here compared with that in reticulocyte lysates or 293T cells transfected with TRPM2-S/TRPM2-L in pcDNA3.1 or pcDNA3.1/V5-His TOPO are results of linkage of GST to TRPM2-S/-L in the pET-42b vector.

To determine whether TRPM2-S directly interacts with TRPM2-L, 293T cells were transfected with empty vector, TRPM2-S in pcDNA3.1/V5-His TOPO, TRPM2-L in pcDNA3.1, or both. Each cell lysate was immunoprecipitated with anti-TRPM2-C to precipitate TRPM2-L or anti-V5 to precipitate TRPM2-S. The blots were probed with anti-TRPM2-C or an-

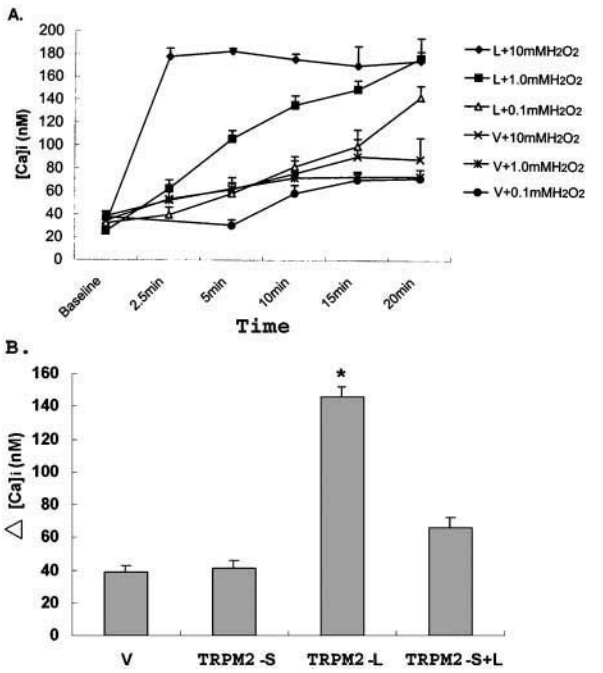

FIG. 7. **Stimulation of Ca^{2+} influx through TRPM2 splice variants by H_2O_2.** 293T cells were transfected with vector alone (pQBI50), TRPM2-S (in pTracer-CMV), TRPM2-L (in pQBI50), or both. 48 h later, successfully transfected single cells were identified by GFP or BFP fluorescence. $[Ca^{2+}]_i$ was measured in Fura Red-loaded, transfected cells at base line and at intervals over 20 min after treatment with H_2O_2. *A*, $[Ca^{2+}]_i$ was measured in 293T cells transfected with vector alone (*V*) or TRPM2-L (*L*) and treated with 0.1, 1.0, or 10 mM H_2O_2. Mean $[Ca^{2+}]_i$ + S.E. is shown. Four to thirteen cells were studied at each H_2O_2 concentration. *B*, the change in $[Ca^{2+}]_i$ is shown in cells transfected with vector alone, TRPM2-S, TRPM2-L, or both following treatment with 1.0 mM H_2O_2 for 20 min. Mean change in $[Ca^{2+}]_i$ + S.E. is shown for 13 (*V*), 16 (*TRPM2-S*), 20 (*TRPM2-L*), or 28 (*TRPM2-S+L*) transfected cells studied. The *asterisk* indicates a significant difference compared with vector alone, TRPM2-S-transfected, and TRPM2-S+L-transfected cells ($p \leq 0.01$).

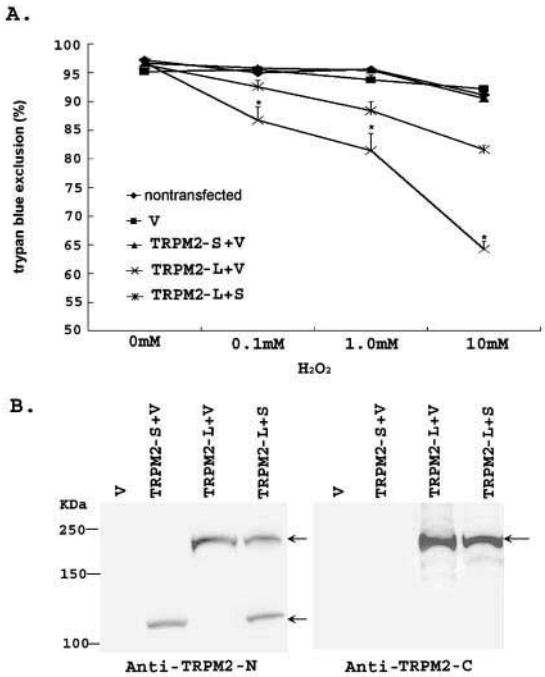

FIG. 8. *A*, viability of cells transfected with TRPM2 splice variants and treated with H_2O_2. 293T cells were transfected with vector alone, TRPM2-S, TRPM2-L, or combinations in pQBI50. Each group of transfected cells was treated with 0, 0.1, 1.0, or 10 mM H_2O_2 for 40 min, and cell viability assessed by trypan blue exclusion. The *asterisk* indicates a significant difference from the other groups of transfected cells ($p \leq 0.01$). Mean trypan blue exclusion + S.E. for three experiments is shown. *B*, Western blot of 293T cells transfected with TRPM2 splice variants. 293T cells were transfected with equivalent amounts of vector alone (pQBI50), TRPM2-S, TRPM2-L, or both. The cell lysates were prepared, and 100 μg of each was loaded in each lane. The blots were probed with anti-TRPM2-N or anti-TRPM2-C and secondary antibody followed by ECL.

ti-V5 antibodies. The results are shown on Fig. 6*B*. Anti-TRPM2-C antibody immunoprecipitated TRPM2-S when TRPM2-L was coexpressed, and anti-V5 antibody immunoprecipitated TRPM2-L in the presence of TRPM2-S, demonstrating the direct interaction of TRPM2-S with TRPM2-L.

TRPM2-S Inhibits Calcium Influx through TRPM2-L—H_2O_2 has previously been demonstrated to evoke calcium influx through TRPM2 and to increase $[Ca^{2+}]_i$ (3, 4). To confirm these results, 293T cells were transfected with empty vector or TRPM2-L in pQBI50. Successful transfection of empty vector or TRPM2-L was confirmed by detection of BFP, fused through a flexible linker to TRPM2-L, in single cells with our digital video imaging system. $[Ca^{2+}]_i$ was measured in these cells by detection of Fura Red fluorescence at base line and at intervals over 20 min following exposure to 0.1, 1, or 10 mM H_2O_2. These experiments confirmed a significant and dose-dependent increase in $[Ca^{2+}]_i$ in TRPM2-L-transfected cells in response to H_2O_2. The increase in $[Ca^{2+}]_i$ in TRPM2-L-transfected cells was significantly greater than that observed in cells transfected with vector alone at all concentrations of H_2O_2 at exposure times of 5 min or greater ($p \leq 0.05$). These results are shown in Fig. 7*A*.

To determine whether TRPM2-S can modulate H_2O_2-induced calcium influx through TRPM2-L, 293T cells were transfected with vector alone, TRPM2-S in pTracer-CMV, TRPM2-L in pQBI50, or both. Successfully transfected individual 293T cells were identified for study by detection of GFP (TRPM2-S), BFP (empty vector, TRPM2-L), or both with our digital video imaging system. $[Ca^{2+}]_i$ was measured in Fura Red-loaded, transfected cells before and at intervals for 20 min after exposure to 1.0 mM H_2O_2. The mean peak increase in $[Ca^{2+}]_i$ above base line for the four groups of transfected cells is shown in Fig. 7*B*. The increase in $[Ca^{2+}]_i$ following treatment with 1.0 mM H_2O_2 in 293T cells transfected with TRPM2-S was not statistically different from vector alone transfected cells. As noted above, the peak increase in $[Ca^{2+}]_i$ in TRPM2-L-transfected cells was significantly greater than that seen in cells transfected with vector alone or TRPM2-S ($p \leq 0.01$). In cells transfected with both TRPM2-L and TRPM2-S, the peak increase in $[Ca^{2+}]_i$ was significantly less than that observed in cells transfected with TRPM2-L alone ($p < 0.001$), demonstrating the ability of TRPM2-S to inhibit calcium influx through TRPM2-L.

TRPM2-S Suppresses Susceptibility to Cell Death Induced through TRPM2 by H_2O_2—TRPM2-expressing cells are susceptible to cell death induced by exposure to H_2O_2 (3). Here, the ability of TRPM2-S to modulate cell death induced by H_2O_2 was examined. 293T cells were transfected with vector alone, TRPM2-S, TRPM2-L, or combinations in pQBI50. Empty vector was transfected with TRPM2-S or TRPM2-L to maintain the equivalent amount of DNA used in cotransfection of both TRPM2-S and TRPM2-L. At 48 h, the cells were treated with 0, 0.1, 1.0, or 10 mM H_2O_2 for 40 min. The cell viability was then assessed by trypan blue exclusion. The results are shown on Fig. 8*A*. Treatment of TRPM2-L-transfected cells with H_2O_2 resulted in a significant and dose-dependent decrease in cell viability compared with untransfected cells, cells transfected with vector alone, or cells transfected with TRPM2-S ($p \leq 0.01$). In 293T cells expressing both TRPM2-S and TRPM2-L,

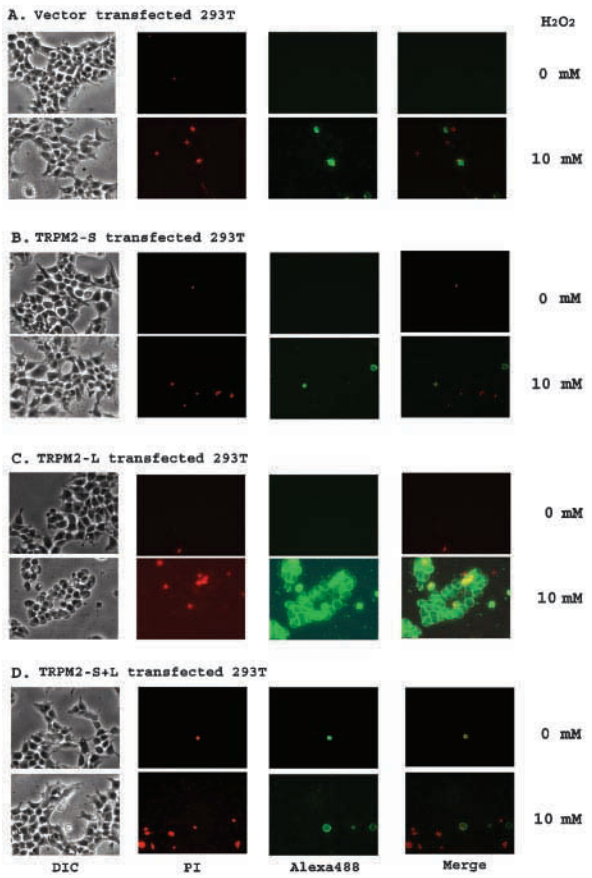

FIG. 9. **Apoptosis in 293T cells transfected with TRPM2 splice variants.** 293T cells were transfected with vector alone (pQBI50, *A*), TRPM2-S (*B*), TRPM2-L (*C*), or TRPM2-S and TRPM2-L in pQBI50 (*D*). The cells were treated with 0 or 10 mM H_2O_2 for 40 min and then incubated with propidium iodide and Alexa Fluor 488/annexin V. Representative white light images of cells (*DIC*), fluorescence of PI, fluorescence of Alexa 488 (Annexin), or the merged image of propidium iodide and Alexa 488 staining are shown for each group of transfected cells.

the cell viability was significantly enhanced compared with TRPM2-L expressing cells ($p \leq 0.001$).

To confirm that this suppression of H_2O_2-induced cell death did not result from decreased expression of TRPM2-L in co-transfected cells, Western blotting was performed on cells transfected with vector alone, TRPM2-S, TRPM2-L, or both in pQBI50 under the same conditions as above for 48 h. The results, shown in Fig. 8*B*, demonstrate nearly equivalent expression of TRPM2-S and TRPM2-L in cells that were transfected with both cDNAs simultaneously when compared with cells transfected with each cDNA alone. The higher molecular masses of proteins shown here compared with that in reticulocyte lysates or 293T cells transfected with TRPM2-S/TRPM2-L in pcDNA3.1 or pcDNA3.1/V5-His TOPO is a result of linkage to BFP.

To assess the ability of TRPM2-S to inhibit apoptosis or necrosis in response to oxidative stress, 293T cells transfected for 48 h with vector alone (pQBI50), TRPM2-S, TRPM2-L, or both were treated with 0 or 10 mM H_2O_2 for 40 min. Apoptosis was assessed by labeling of cells with Alexa Fluor 488 annexin V conjugates; annexin V binds to phosphatidylserine on the surface of early apoptotic cells. Necrosis was assessed by labeling with propidium iodide, which binds to nucleic acids in necrotic cells but does not penetrate live cell membranes or early apoptotic cells. Representative results are shown in Fig. 9. Treatment of 293T cells transfected with vector alone (Fig. 9*A*) or with TRPM2-S (Fig. 9*B*) with 0 or 10 mM H_2O_2 resulted in barely detectable apoptosis (Alexa 488 annexin) or necrosis (PI). In contrast, 293T cells transfected with TRPM2-L demonstrated little apoptosis or necrosis with vehicle (0 mM H_2O_2) but $\geq$70% apoptotic cells when treated with 10 mM H_2O_2 (Fig. 9*C*). When 293T cells were transfected with both TRPM2-S and TRPM2-L, the number of apoptotic cells was greatly reduced (<10%) compared with cells transfected with TRPM2-L alone (Fig. 9*D*). Necrosis was not a prominent finding in any of these H_2O_2-treated cells after 40 min. Three experiments were performed with similar results.

DISCUSSION

In this report, a new isoform of TRPM2, TRPM2-S, was cloned from human bone marrow and consists of only the N terminus and the first two transmembrane domains. Here, we demonstrated that expression of TRPM2-S inhibits calcium influx, enhances cell viability, and reduces apoptosis and cell death, which occur following exposure of full-length TRPM2-expressing cells to H_2O_2. Because H_2O_2 causes an increase in intracellular calcium that precedes cell death in numerous cell types including cardiac and smooth muscle cells, macrophages, and neurons (1), TRPM2-S may have a generally important role in the determination of cell fate following exposure to oxidative stress.

The first major finding of this report is the identification of a short isoform of TRPM2 expressed physiologically in human hematopoietic cells. This is the third TRPM family member for which a short isoform has been identified and is similar to the short isoforms of MLSN (TRPM1) (10) and MTR1 (TRPM5) (12) in that all have a deletion of the C terminus including transmembrane domains and the putative calcium-permeable pore region. N-terminal fragments of *Drosophila* and mammalian TRPCs have previously been shown to bind to and suppress the activity of full-length TRPC proteins (26–28). These N-terminal domains of TRPC were found to participate in heteromultimer complex formation. The physiological short form of MLSN, MLSN-S, which has no transmembrane domains, interacts with and suppresses the activity of full-length MLSN (MLSN-L) (10). MLSN-L localizes near or in the plasma membrane, whereas MLSN-S is uniformly distributed in the cytoplasm. Published data suggest that the suppression of activity by MLSN-S results from direct interaction of MLSN-S and MLSN-L, inhibiting translocation of MLSN-L to the plasma membrane (10). Here we identified a short isoform of TRPM2 that interacts with and suppresses the activity of full-length TRPM2, but the mechanism does not appear to be the same as reported for MLSN-S. Although TRPM2-S directly interacts with TRPM2-L, our experiments demonstrate that TRPM2-S and TRPM2-L have a similar subcellular localization and that TRPM2-S does not alter the localization of TRPM2-L. Unlike MLSN-S, TRPM2-S retains two transmembrane domains that localize it to the cell membrane.

The second major finding of this report is that TRPM2-S is able to inhibit calcium influx induced by H_2O_2 through full-length TRPM2. TRPM2 has been shown to be regulated by at least three different mechanisms. 1) TRPM2 has a Nudix box in its C terminus that has homology to NUDT9, an ADP-ribose pyrophosphatase degrading ADP-ribose (ADPR). Although it can function as an ADPR pyrophosphatase, it has a much lower level of activity than NUDT9 (11). The Nudix box may also serve as an ADPR-binding site, and ADPR has been shown to directly gait TRPM2 opening (11, 17). Because in oxidative stress ADPR production is increased (29), this is a mechanism through which H_2O_2 may regulate TRPM2-L. 2) NAD has also been shown to directly activate TRPM2 (3, 17), although one group of investigators was unable to show that NAD stimulates current through TRPM2 (4). 3) H_2O_2, but not ADPR or NAD,

was able to stimulate calcium influx through an TRPM2 mutant with a small deletion in the C terminus (4). These data suggest that H_2O_2 and oxidative stress can mediate calcium influx through a third mechanism independently of ADPR or NAD. This pathway will need to be defined before the mechanism through which TRPM2-S inhibits H_2O_2-mediated calcium influx through TRPM2-L can be identified. Because TRPCs have been proposed to function as homo- or heterotetramers (30) and TRPM2-S and TRPM2-L are shown here to directly interact, TRPM2-S may participate in heterotetramer formation, altering the tertiary structure of the TRPM2-L homotetramer and inhibiting calcium permeability. Alternatively, because it is missing the C terminus, TRPM2-S could also function to impair localization of TRPM2-L to signaling complexes (6) or act as a dominant negative blocking an unknown aspect of TRPM2-L regulation critical for calcium channel activation.

The third and most important finding of this report is that TRPM2-S inhibits the decreased cell viability and increased susceptibility to cell death that result from activation of TRPM2-L by oxidative stress. Our observation that exposure of TRPM2-L-expressing cells to H_2O_2 reduces cell viability and enhances apoptosis is consistent with previous reports (3, 17). The significance of our work is the identification of a physiological splice variant of TRPM2, which suppresses cell death in response to oxidative stress. The genomic sequence of TRPM2 spans 32 exons (16), raising the possibility that multiple splice variants with different capabilities may exist. In fact, two other splice variants of TRPM2 have been identified in granulocytes and undifferentiated HL-60 cells, which have small deletions in their N terminus (amino acids 538–557) or C terminus (amino acids 1292–1325) (4). H_2O_2 does not induce calcium influx in cells transfected with the N-terminal deletion but is effective in stimulating calcium influx through the C-terminal deletion. No functional studies were performed to examine isoform interactions or the impact of expression of these variants on cell viability. As suggested by our work with TRPM2-S, expression or activation of different isoforms of TRPM2 may be a mechanism through which cells can control their reaction to damaging oxidants. In this event, regulation of splicing of TRPM has important implications for controlling the onset of apoptosis or cell death in response to oxidative stress and needs to be explored. Reduction of TRPM2 levels with antisense oligonucleotides also suppressed $[Ca^{2+}]_i$ oscillations and cell death induced by tumor necrosis factor α in RIN-5F cells and the monocyte cell line U937 (3). This suggests that the level of TRPM2 expression, as well as the ratio of isoforms expressed (TRPM2-S *versus* TRPM2-L), may be important in regulating the proliferative or apoptotic response to stimulation with or withdrawal of certain hematopoietic growth factors. This possibility is being pursued.

In summary, we have identified a physiologic splice variant of TRPM2 that is expressed in hematopoietic cells and interacts directly with full-length TRPM2. Using 293T cells cotransfected with TRPM2-S and TRPM2-L, we demonstrated the ability of TRPM2-S to inhibit H_2O_2-induced calcium influx through TRPM2-L and to suppress the susceptibility to cell death induced through TRPM2-L by H_2O_2. Our studies suggest that TRPM2-S may have an important role in many tissues because it can modulate calcium influx and cellular responses to oxidative stress.

REFERENCES

1. Herson, P. S., Lee, K., Pinnock, R. D., Hughes, J., and Ashford, M. L. (1999) *J. Biol. Chem.* **274,** 833–841
2. Klonowski-Stumpe, H., Schreiber, R., Grolik, M., Schulz, H. U., Haussinger, D., and Niederau, C. (1997) *Am. J. Physiol.* **272,** G1489–G1498
3. Hara, Y., Wakamori, M., Ishii, M., Maeno, E., Nishida, M., Yoshida, T., Yamada, H., Shimizu, S., Mori, E., Kudoh, J., Shimizu, N., Kurose, H., Okada, Y., Imoto, K., and Mori, Y. (2002) *Mol. Cell* **9,** 163–173
4. Wehage, E., Eisfeld, J., Heiner, I., Jungling, E., Zitt, C., and Luckhoff, A. (2002) *J. Biol. Chem.* **277,** 23150–23156
5. Harteneck, C., Plant, T. D., and Schultz, G. (2000) *Trends Neurosci.* **23,** 159–166
6. Montell, C. (2001) *Science's STKE* **2001,** RE1
7. Montell, C., Birnbaumer, L., and Flockerzi, V. (2002) *Cell* **108,** 595–598
8. Duncan, L. M., Deeds, J., Hunter, J., Shao, J., Holmgren, L. M., Woolf, E. A., Tepper, R. I., and Shyjan, A. W. (1998) *Cancer Res.* **58,** 1515–1520
9. Hunter, J. J., Shao, J., Smutko, J. S., Dussault, B. J., Nagle, D. L., Woolf, E. A., Holmgren, L. M., Moore, K. J., and Shyjan, A. W. (1998) *Genomics* **54,** 116–123
10. Xu, X. Z., Moebius, F., Gill, D. L., and Montell, C. (2001) *Proc. Natl. Acad. Sci. U. S. A.* **98,** 10692–10697
11. Perraud, A. L., Fleig, A., Dunn, C. A., Bagley, L. A., Launay, P., Schmitz, C., Stokes, A. J., Zhu, Q., Bessman, M. J., Penner, R., Kinet, J. P., and Scharenberg, A. M. (2001) *Nature* **411,** 595–599
12. Prawitt, D., Enklaar, T., Klemm, G., Gartner, B., Spangenberg, C., Winterpacht, A., Higgins, M., Pelletier, J., and Zabel, B. (2000) *Hum. Mol. Genet.* **9,** 203–216
13. Tsavaler, L., Shapero, M. H., Morkowski, S., and Laus, R. (2001) *Cancer Res.* **61,** 3760–3769
14. Runnels, L. W., Yue, L., and Clapham, D. E. (2001) *Science* **291,** 1043–1047
15. Paulsen, M., El Maarri, O., Engemann, S., Strodicke, M., Franck, O., Davies, K., Reinhardt, R., Reik, W., and Walter, J. (2000) *Hum. Mol. Genet.* **9,** 1829–1841
16. Nagamine, K., Kudoh, J., Minoshima, S., Kawasaki, K., Asakawa, S., Ito, F., and Shimizu, N. (1998) *Genomics* **54,** 124–131
17. Sano, Y., Inamura, K., Miyake, A., Mochizuki, S., Yokoi, H., Matsushime, H., and Furuichi, K. (2001) *Science* **293,** 1327–1330
18. Zhang, M. Y., Harhaj, E. W., Bell, L., Sun, S. C., and Miller, B. A. (1998) *Blood* **92,** 1225–1234
19. Vannier, B., Peyton, M., Boulay, G., Brown, D., Qin, N., Jiang, M., Zhu, X., and Birnbaumer, L. (1999) *Proc. Natl. Acad. Sci. U. S. A.* **96,** 2060–2064
20. Hofmann, T., Obukhov, A. G., Schaefer, M., Harteneck, C., Gudermann, T., and Schultz, G. (1999) *Nature* **397,** 259–263
21. Chu, X., Cheung, J. Y., Barber, D. L., Birnbaumer, L., Rothblum, L. I., Conrad, K., Abrasonis, V., Chan, Y. M., Stahl, R., Carey, D. J., and Miller, B. A. (2002) *J. Biol. Chem.* **277,** 34375–34382
22. Miller, B. A., Barber, D. L., Bell, L. L., Beattie, B. K., Zhang, M. Y., Neel, B. G., Yoakim, M., Rothblum, L. I., and Cheung, J. Y. (1999) *J. Biol. Chem.* **274,** 20465–20472
23. Miller, B. A., Cheung, J. Y., Tillotson, D. L., Hope, S. M., and Scaduto, R. C., Jr. (1989) *Blood* **73,** 1188–1194
24. Cheung, J. Y., Elensky, M. B., Brauneis, U., Scaduto, R. C., Jr., Bell, L. L., Tillotson, D. L., and Miller, B. A. (1992) *J. Clin. Invest.* **90,** 1850–1856
25. Cheung, J. Y., Zhang, X. Q., Bokvist, K., Tillotson, D. L., and Miller, B. A. (1997) *Blood* **89,** 92–100
26. Xu, X. Z., Chien, F., Butler, A., Salkoff, L., and Montell, C. (2000) *Neuron* **26,** 647–657
27. Balzer, M., Lintschinger, B., and Groschner, K. (1999) *Cardiovasc. Res.* **42,** 543–549
28. Xu, X. Z. S., Li, H.-S., Guggino, W. B., and Montell, C. (1997) *Cell* **89,** 1155–1164
29. Wilson, H. L., Dipp, M., Thomas, J. M., Lad, C., Galione, A., and Evans, A. M. (2001) *J. Biol. Chem.* **276,** 11180–11188
30. Birnbaumer, L., Boulay, G., Brown, D., Jiang, M., Dietrich, A., Mikoshiba, K., Zhu, X., and Qin, N. (2000) *Recent Prog. Horm. Res.* **55,** 127–162